A New Hybrid Sensorimotor Driver Model with Model Predictive Control

Kazuhide Okamoto
School of Aerospace Engineering
Georgia Institute of Technology
Atlanta, Georgia 30332–0150
Email: kazuhide@gatech.edu

Panagiotis Tsiotras
School of Aerospace Engineering
Atlanta, Georgia 30332–0150
Email: tsiotras@gatech.edu

***Abstract*—Many driver models assume that a human driver can be modeled as a linear time-invariant system. Although during specific execution tasks this can be a reasonably good model, in general, this is an unrealistic and quite restrictive assumption for most real-life situations where more complex cognitive functions need to be evoked, such as long-term, deliberative planning, prioritization among several possible alternatives, etc. In this paper we model a human driver as a hybrid controller that switches between long-term, discrete planning tasks and short-term, continuous trajectory tracking tasks. The new driver model is based on the well-known two-point visual driver model, and it uses a model predictive control (MPC) module in the anticipatory control channel to better predict deliberative, human driver actions. We evaluate this model's performance, and compare it with other driver models using numerical simulations. The results show that the proposed new driver model reacts to the variation of the direction angle in the same way as most human drivers do, and outperforms previous similar driver models.**

I. Introduction

A number of studies have focused on advanced driver assist systems (ADAS) such as adaptive cruise control (ACC), automatic braking system (ABS), collision avoidance system (CAS), driver monitoring system (DMS) etc, with the aim of increasing safety and mitigating driver's workload. These systems have become standard in most current commercial passenger vehicles. However, the application of ADAS is still restricted to relatively simple tasks, such as following the vehicle ahead or initiating emergency braking in front of an unexpected obstacle. To assist human drivers react in more complex situations, future ADAS will require a more thorough understanding of common human driver behavior, as well as the ability to interpret human driver intent, necessitating a more comprehensive investigation of human driver models.

Researchers have investigated human driver modeling for many decades, dating back to 1938 with the pioneering research by Gibson and Crooks [1]. See [2] for a recent overview. More relevant to the work in this paper is the model by Salvucci and Gray [3] who proposed the so-called two-point visual driver model, depicted in Fig. 1. This model assumes that a human driver processes visual information by concentrating her gaze on two points, namely, the so-called "close ahead" point and the "far ahead" point while driving. Sentouh et al. [4] further developed this model, and incorporated human sensorimotor activity. Using this two-point visual model, the authors in [5] evaluated the performance of an ADAS, while in [6] a steering assist system was designed for lane-keeping tasks.

978-1-5090-1897-0/16/$31.00 ©2016 IEEE

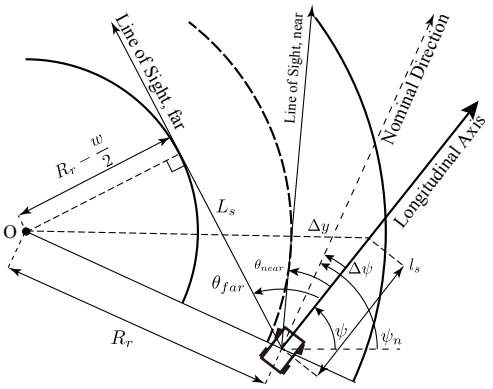

Fig. 1: Two-Point Visual Driver Model

Many of existing driver models, including the two-point visual model, use transfer functions to process the visual input signal. However, transfer functions may not be suitable for modeling certain human brain functions, in particular, high level cognitive tasks. For example, it is commonly known that humans respond to external stimuli in two distinct ways: unconsciously/involuntarily and deliberatively. Based on internal models of the environment, humans have the ability to predict the results of their actions in the near future [7]. In other words, initiating an action often entails an element of optimization in the human brain, especially in cases not encountered before, where prior knowledge and experience may be of little help.

To implement this "optimal" control (re)action, in this paper we incorporate model predictive control (MPC) into the sensorimotor two-point visual driver model [4]. In the proposed model, the MPC controller operates *only* on the anticipatory control channel of the control action, mimicking the human brain activity that processes signals from the eyes, in order to anticipate the vehicle trajectory in the near future and calculate the corresponding control output. MPC is favorable for our objective, because it can explicitly express the difference between different driving styles. For example, when turning along a curve, some people try to stay at the center of the road, while others drive close to the inner edge. A plausible explanation for this difference in driving style is the different optimization criteria used between different drivers, different

optimization parameters or different optimization horizons.

Many researchers have investigated prediction of drivers' behavior [8], [9], [10] and modeling and characterization of drivers [11], [12] from sensory data. Previous research on steering control using MPC includes [13], [14]. Wei et al. [15] compared the performance of a driver model using MPC with a driver model using an artificial neural network (ANN), and showed superior performance of an ANN based-model in reproducing a professional human driver's control action in a closed circuit. However, ANN training requires a large amount of data. Also, it is in general hard to interpret resulting structures of ANN, i.e., the number of hidden layers, the weights and the biases of each node.

In this paper, we develop a driver model using MPC, but contrary to similar prior MPC-based models, we use MPC in an asynchronous matter, namely only for optimization to generate periodically feedforward, anticipatory control actions. As such, it is not necessary to re-optimize often; instead, a compensatory control element ensures that good tracking performance is maintained. The proposed driver model combines discrete deliberative action, provided by the anticipatory channel of the two-point visual driver model, and continuous control action through the compensatory channel. The resulting driver model is therefore a hybrid controller [16] that combines a continuous transfer function-based controller and a discrete-time optimization-based controller. This hybrid nature of the model enables the reproduction of human driver behavior in a realistic manner.

II. Driver Modeling

The driver-vehicle system used in this work consists of four subsystems, as shown in Fig. 2: the steering column, the vehicle, the perception and vision kinematics, and the driver. The steering column and vehicle dynamics subsystems are the same as the ones used in [5]. Specifically, a bicycle model with linear tire friction dynamics is used as the vehicle model, and a first order model with damping is used to model the interface between the driver and the vehicle, including the alignment torque from the vehicle as shown in Fig. 2. The visual perception and driver subsystems are less standard and are described in greater detail below.

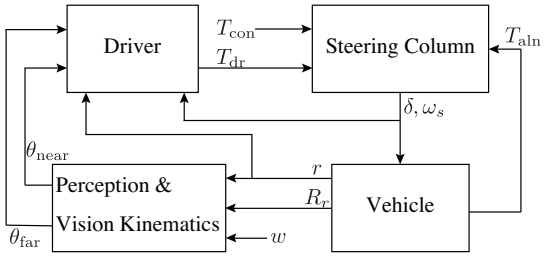

Fig. 2: Vehicle Driver Interaction

A. Visual Perception Model

The perception and vision kinematics subsystem describes how human drivers perceive visual cues from the road geometry. As shown in Fig. 2, the inputs are the yaw rate r, the turning radius R_r, and the road width w. The outputs are the visual perception signals of the driver, namely, the angles $\theta_{\rm near}$ and $\theta_{\rm far}$. According to [17], when humans steer, they look at a point tangent to the inner edge of the curve. We represent this with the "Line of Sight, far" in Fig. 1. From the geometry, $L_s = \sqrt{R_r^2 - (R_r - w/2)^2}$, and we can calculate the far away gaze direction angle as $\theta_{\rm far} = \Delta\psi + \arcsin(L_s/R_r)$, where $\Delta\psi$ is the angle between the nominal and actual vehicle yaw angle $\Delta\psi = \psi_n - \psi$. Fig. 1 also shows $\theta_{\rm near}$, the angle between the "Line-of-Sight, near" vector and the longitudinal axis of the vehicle. We assume that the length ℓ_s is a constant. Since $\theta_{\rm near}$ is small, $\theta_{\rm near} \approx (\Delta y/\ell_s)$, where Δy is governed by $\Delta\dot{y} = -V_x(\beta - \Delta\psi) - \ell_s r + V_x \ell_s / R_r$.

B. Driver

The inputs of the driver subsystem are the visual cues of the road from the vision kinematics, $\theta_{\rm near}$ and $\theta_{\rm far}$, the steering angle δ and steering angle rate ω_s, and the vehicle yaw rate r. The output is the driver steering torque $T_{\rm dr}$. Fig. 3 shows the four main components of this model: the neuromuscular subsystem, the delay, the compensatory control subsystem, and the anticipatory control subsystem. The gate before the anticipatory control explicitly represents the fact that the anticipatory control block can acquire observation information only at a certain time intervals. The neuromuscular subsystem models the human arm movement as a transfer function $G_{\rm nm}(s) = 1/(T_N s + 1)$, where T_N is a constant. The delay captures the time lag of human brain's sensory signal processing and is given by $G_L(s) = e^{-t_p s}$, where t_p is a constant. The compensatory control generates the correction torque $T_{\rm comp}$, based on the input near-angle $\theta_{\rm near}$. $G_c(s) = K_c(T_L s + 1)/(T_I s + 1)$, where $T_L > T_I$, and K_c is a gain. For a detailed description of these blocks, the reader is referred to [4] and [5].

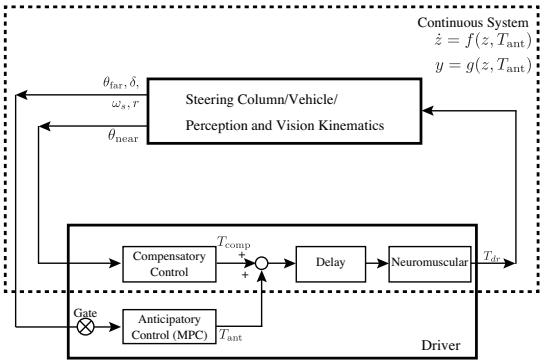

Fig. 3: Description of the driver model

The compensatory control subsystem corresponds to the unconscious response by the nervous system. The anticipatory control subsystem generates and tracks the reference trajectory at a distant future time instant. We hypothesize that this corresponds to brain activity, by which the brain processes signals from the sensory organs, anticipates the future, and sends signals to muscles. In [4], the authors used a transfer function to model this anticipatory control. This work assumes that the

anticipatory control can be better modeled by incorporating a periodic optimal control action.

The sensori-motor driver model has a compensatory control $T_{\rm comp}$ element and an anticipatory control $T_{\rm ant}$ element, which are combined to produce the driver's steering torque $T_{\rm dr}$ as

$$T_{\rm dr} = G_{\rm nm} G_L (T_{\rm comp} + T_{\rm ant}). \tag{1}$$

Note that both $T_{\rm ant}$ and $T_{\rm comp}$ are state-feed back controllers, but while $T_{\rm comp}$ is a continuous-time control input, $T_{\rm ant}$ is a discrete-time control input calculated at every pre-determined sampling time step, and that in this time interval, $T_{\rm ant}$ is assumed to be constant.

C. Two-Point Driver Model as a Hybrid System

In this section, we propose a driver model using a hybrid system modeling framework [16]. A hybrid system is defined by

$$\begin{cases} \dot{x} = F(x), & x \in C, \\ x^+ = G(x), & x \in D, \end{cases} \tag{2}$$

where $C \subseteq \mathbb{R}^n$ is the flow set, $F : \mathbb{R}^n \to \mathbb{R}^n$ is the flow map, $D \subseteq \mathbb{R}^n$ is the jump set, and $G : \mathbb{R}^n \to \mathbb{R}^n$ is the jump map. In (2) $\dot{x}$ and x^+ represent the derivative of x, and the value of x after an instantaneous change, respectively. The state $x \in \mathbb{R}^n$ is governed by F when $x \in C$, and "jumps" when $x \in D$ according to G.

Suppose the steering column, vehicle, and perception and vision kinematics subsystems, combined with the road, vehicle, steering column, vision, neuromuscular activity, signal processing delay, and compensatory control subsystems can be represented using the equations

$$\dot{z} = f(z, T_{\rm ant}) \tag{3}$$

$$y = g(z, T_{\rm ant}) \tag{4}$$

where $z \in \mathbb{R}^{n_z}$ is the state of the system, and $y = (\theta_{\rm near}, \delta, \omega_s, r)$ is the output (see also Fig. 3).

The gate subsystem in Fig. 3 passes the observation signal only when the inner variable τ reaches a pre-specified time determined by the gate sampling rate t_s. The variable τ evolves as $\dot{\tau} = 1$. Let the overall state variable be defined by $x = (z, T_{\rm ant}, \tau)$. We can then formulate the problem as a hybrid system as follows: Flow occurs when $\tau \in [0, t_s)$. During flow $T_{\rm ant}$ remains constant, τ keeps track of elapsed time, and the state z evolves based on the dynamics $\dot{z} = f(z, T_{\rm ant})$. Consequently, the flow set is $C = \mathbb{R}^{n_z} \times \mathbb{R} \times [0, t_s)$ and the flow map is $F(x) = (f(z, T_{\rm ant})^\intercal, 0, 1)^\intercal$ At jumps, the anticipatory control $T_{\rm ant}$ is updated based on a receding horizon optimization, as explained in Section III. We denote this new anticipatory control input as $T^*_{\rm ant}$. Note that at jumps, the gate's inner variable τ is reset to 0, and the state z does not change. Therefore, the jump set is $D = \mathbb{R}^{n_z} \times \mathbb{R} \times \{t_s\}$ and the jump map is $G(x) = (z^\intercal, T^*_{\rm ant}, 0)^\intercal$.

III. MPC Design

In the proposed driver model, we calculate $T_{\rm ant}$ periodically with MPC. MPC predicts the future state of the system and calculates the control that minimizes the given objective function. Let the current time be $t_0 = kt_s$ at the kth iteration of the MPC algorithm. Also, let the time horizon be Nt_s. The optimization problem to be solved is

$$\text{find} \quad T_{\rm ant}(t), \quad t_0 \le t \le t_h \tag{5}$$

to minimize

$$J = \int_{t_0}^{t_h} (Q_\omega \omega_s^2 + R_T T_{\rm ant}^2)\, {\rm d}t, \tag{6}$$

where $t_h = (k+N)t_s$, subject to the prediction of the vehicle's movement, the internal signal processing architecture, and the boundary condition so that the direction angle at the end of the horizon $\psi(t_h)$ is the sum of $\theta_{\rm far}$ and the current direction angle $\psi(t_0)$ (see Fig. 1):

$$\psi(t_h) = \psi(t_0) + \theta_{\rm far}(t_0). \tag{7}$$

In (6) the variables Q_ω and R_T represent cost weights. We use $\theta_{\rm far}(t_0)$ in (7) to emphasize the fact that the driver has access to $\theta_{\rm far}$ only when the gate opens. Note that since the driver does not have access to the side-slip angle β, we assume $\beta(t_0) \approx 0$. Without loss of generality, we may set $\psi(t_0) = 0$ since we only care about the difference in the heading direction $\psi(t) - \psi(t_0)$. This is equivalent to the fact that human drivers do not change their steering action depending on the inertial driving direction. Condition (7) encodes the hypothesis that when human drivers see the "far-ahead" point, they infer the desired/predicted vehicle direction angle at a future time.

Since MPC is a discrete-time control methodology, we discretize the dynamics (3), which in our problem setting is linear, with sampling period t_s to obtain

$$\boldsymbol{x}_d(h+1) = A^d \boldsymbol{x}_d(h) + B^d \boldsymbol{u}_d(h) \tag{8}$$

where h is time step index, $\boldsymbol{x}_d = (\omega_s, \delta, \beta, r, \psi, x_{\rm dr}^\intercal)^\intercal$, $\boldsymbol{u}_d = T_{\rm ant}$, and $x_{\rm dr}$ is internal state vector of the driver. Consequently, we formulate the MPC problem as follows

$$\begin{aligned} J = {} & P_\psi (\psi(N) - \psi(0) - \theta_{\rm far}(t_0))^2 \\ & + \sum_{h=0}^{N-1} \left[Q_\omega \omega_s(h)^2 + R_T T_{\rm ant}(h)^2 \right], \end{aligned} \tag{9}$$

subject to

$$\boldsymbol{x}_d(h+1) = A^d \boldsymbol{x}_d(h) + B^d \boldsymbol{u}_d(h), \tag{10}$$

$$\boldsymbol{u}_{\min} \le \boldsymbol{u}(h) \le \boldsymbol{u}_{\max}, \ h = 0, \dots, N_u - 1 \tag{11}$$

$$\boldsymbol{u}(h) = 0, \ h = N_u, \dots, N-1 \tag{12}$$

where P_ψ, Q_ω, and R_T are given weights, $U_N(k) = (u(0), \dots, u(N-1))$, N is the prediction horizon, and N_u is the control constraint horizon. The first term in (9) is the discretized boundary condition (7), and the ω_s term is to reduce oscillation in the solution. While $t_0 \le t \le t_0 + t_s$, $T_{\rm ant}$ is a constant, and when $t = t_0 + t_s$, $T_{\rm ant}$ is updated. The resulting output from the driver subsystem, $T_{\rm dr}$ is calculated as in (1).

TABLE I: The vehicle and the steering system parameters. (C.G.: The vehicle's center of gravity.)

Parameter, Unit	Notation	Value
Mass, kg	m	1,653
Distance from C.G. to the Front Axis, m	l_f	1.402
Distance from C.G. to the Rear Axis, m	l_r	1.646
Moment of Inertia, kg $\cdot$ m^2	I_z	2,765
Front Tires Cornering Power, N/rad	C_f	42,000
Rear Tires Cornering Power, N/rad	C_r	81,000
Width of the Tire Contact, m	n_t	0.225
Steering System Axis Inertia, kg $\cdot$ m^2	J_s	0.11
Steering Gear Friction, N $\cdot$ m/rad/s	B_s	0.57
Manual Steering Column Coefficient	K_p	0.038

IV. Numerical Simulations

In this section, we evaluate the performance of the proposed driver model using numerical simulations. We conducted simulations with Simulink, used the Hybrid Toolbox [18] to implement MPC, and employed CarSim [19] to reproduce the dynamic motion of a vehicle. Note that although we used the simplified bicycle model for controller design, we evaluated the performance using CarSim's internal high-fidelity vehicle model. Table I shows the vehicle and the steering subsystem parameters. Also, the driver parameters are $T_N = 0.12$, $t_p = 0.04$, $K_c = 18$, $T_L = 2.8$, and $T_I = 0.18$. In all the simulations, we set the cost weights in (9) as $P_\psi = 2.7 \times 10^3$, $Q_\omega = 2.0$, and $R_T = 1.0$.

A. Straight Road

First, we examined the proposed driver model's corrective behavior while driving straight. Hildreth et al. [20] conducted several experiments to reveal the characteristics of human drivers. Salvucci and Gray successfully reproduced these characteristics in their driver model using numerical simulations [3]. Here, we show that the proposed model can also exhibit the same tendency of human drivers. This simulation consists of two numerical experiments. The first experiment assesses the effect of the initial heading angle deflection. We investigate the model behavior subject to various initial settings of the heading angle. In the second experiment, we fix the initial heading angle of the vehicle and investigate the difference of steering behavior with changing vehicle speed.

1) Effect of Initial Heading Angle Deviation: The first experiment investigates the effect of the vehicle heading on the steering wheel angle profiles. We fix the vehicle speed to 25 m/s, change the initial direction angle, and observe the driver's steering column angle profile. The settings of the initial heading angle are $1.0°$, $1.5°$, $2.0°$, $2.5°$, and $3.0°$. Fig. 4 shows the time history of the steering wheel angle. We set the sampling period as $t_s = 0.5$ sec, and after each time step, MPC re-calculates the optimal control. Also, we set $N = 4$ and $N_u = 2$. Therefore, MPC calculates the trajectory of the system over the next 2 sec. In [20], Hildreth et al. revealed that humans use larger steering wheel angle magnitude when the initial vehicle heading angle is larger, but the time spent for correction does not change much. Our results successfully reproduced this tendency: Although the driver took around $32°$ of steering wheel angle magnitude to correct the $3°$ deflection and $7°$ of steering angle to correct $1°$, the first reaction of all the cases took around 1 sec.

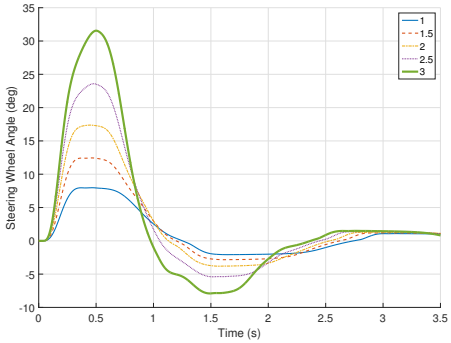

Fig. 4: Corrective steering angle profile varying the initial heading of the vehicle.

2) Effect of Speed: In the second numerical experiment, we investigated the effect of speed over the steering action. Here, we fix the vehicle's initial heading angle deflection at $2.0°$, and changed the vehicle speed. We employed the following five speed settings: 17.5, 20.0, 22.5, 25.0 and 27.5 m/s. According to [20] human drivers tend to complete a corrective maneuver in shorter time when the vehicle speed is faster, but the magnitude of steering does not change much. The original two-point visual driver model succeeded in capturing this tendency. Fig. 5 shows that the model successfully captured this tendency as well: In all the settings, the magnitude of the first reaction was around $17°$, but when the speed was 27.5 m/s the driver model took the shortest time, and when the speed was 17.5 m/s the driver took the longest time.

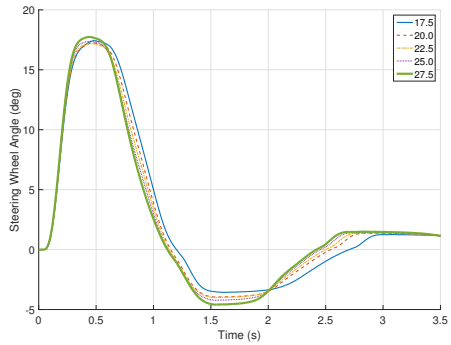

Fig. 5: Corrective steering angle profile varying the speed of the vehicle.

B. Closed Circuit

In the previous scenario, we observed that the proposed driver model can reproduce the tendency of human drivers to correct the direction angle deflection. Next, we evaluate and compare the performance of the proposed driver model with other models. We denote the proposed driver model DRV1. We also employ another MPC-based driver model that does not have the compensatory control part. Instead,

DRV2 calculates the optimal control action sequence at higher frequency, namely, 100 Hz. We call this model DRV2. In order to follow the center of the course, we set the cost function for DRV2 as follows

$$J_2 = P_\psi(\psi(N) - \psi(0) - \theta_{\rm far}(t_0))^2 + \sum_{h=0}^{N-1} \left[Q_\omega \omega_s(h)^2 + Q_{\Delta y}\Delta y(h)^2 + R_T T_{\rm ant}(h)^2\right]. \quad (13)$$

We select the cost weights as $P_\psi = 2.7 \times 10^3$, $Q_\omega = 2.0$, $Q_{\Delta y} = 1.0 \times 10^3$, and $R_T = 1.0$. Since the optimal control is calculated at 100 Hz, the sampling period is set to be 0.01 sec. Therefore, for DRV2 we choose $N = 200$ and $N_c = 100$ to have the same prediction horizon: 2 sec.

Furthermore, we employ a transfer function-based sensorimotor two-point visual driver model. We call this model DRV3. All the parameters are the same as before, except for the anticipatory control, for which DRV3 employs the following function: $T_{\rm ant} = K_a \theta_{\rm far}(t)$, where $K_a = 28$. Note that $\theta_{\rm far}$ is a function of t, not t_0, since this anticipatory control is not a discrete-time controller.

Finally, we employ a sensorimotor driver model in which the driver does not use $\theta_{\rm far}$ for steering ($K_a = 0$). This results in a one-point visual driver model that lacks the anticipatory control component. We call this driver DRV4.

The numerical tests were conducted using one of CarSim's built-in closed circuits, whose length is 2.2 km, shown in Fig. 6. During the simulation the vehicle speed is kept constant at 50 km/h ≈13.89 m/s, while the driver tries to follow the center of the road. This scenario is rather challenging because the path consists of both right and left corners having various turning radii and straight lines, which the drivers have to deal with. as they drive at high speed along the course.

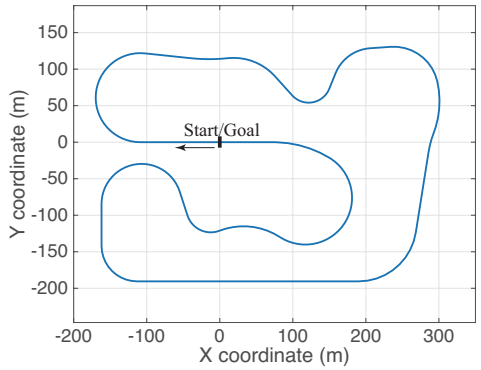

Fig. 6: Course used for simulation.

Fig. 7 shows the root mean square (RMS) of each driver model's deviation after one lap. The smaller the value, the better the performance. One can easily see the poor performance of DRV4, which had difficulty following the path. DRV1, DRV2, and DRV3 exhibited almost the same amount of RMS deviation. But at steep turns both the DRV1 and DRV2 outperformed DRV3. Furthermore, thanks to its hybrid nature, DRV1 could exhibit equivalent performance to DRV2 (another MPC-based driver model) while optimizing less frequently (DRV1: 2 Hz, DRV2:100 Hz). The high optimization frequency of DRV2 is, however, unrealistic for human drivers. We note that DRV2 could not stay in course when the optimization frequency was reduced to 2 Hz. These results show that implementing a hybrid dynamical system of MPC and a continuous transfer function-based controller is a realistic methodology to reproduce human drivers' steering behavior.

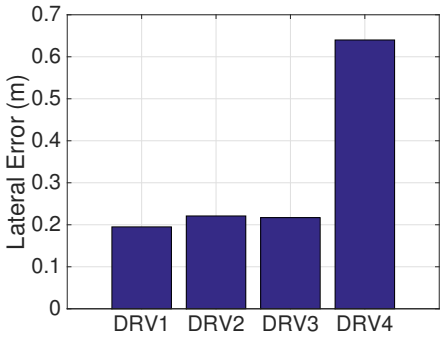

Fig. 7: RMS of lateral error from the center line of the road.

C. Parameter Study

In this section, we perform several parameter studies of the proposed driver in order to investigate the effect of the sampling period t_s and the optimization horizon t_h. For simplicity, we let $t_0 = 0$ and denote the time horizon as t_h in this discussion. Experienced drivers, presumably, have the ability to cope with the changes of the environment more quickly and to predict longer future than novice drivers. The sampling period corresponds to how often the human driver re-computes the steering torque while driving. The smaller the value, the more often the driver recalculates the future steering output. Larger values of t_h correspond to human drivers who can predict the future vehicle trajectory longer. Therefore, intuitively, driver models should have better performance when t_s is short, and t_h is long.

Fig. 8a shows the time history of lateral error of four driver models with different settings of $t_s = 0.1,\ 0.5,\ 1.0$, and 2.0 sec. The time horizon t_h is fixed to be 2 sec in all cases. For simplicity, we abbreviate t_0 and denote the time horizon as t_h in this discussion. Fig. 8b depicts the lateral error profile during one lap with the following four different settings: $t_h = 1.0,\ 2.0,\ 3.0$, and 5.0 sec. The sampling period is fixed at $t_s = 0.5$ sec. These results show that the performance of the overall model does not necessarily increase by increasing the optimization frequency or increasing the time-horizon. This is owing to the fact that we have formulated the problem such that the anticipatory (MPC) control objective and the compensatory control objective are not quite aligned. Specifically, as shown in (9), the anticipatory control subsystem does not take into account $\theta_{\rm near}$, the measure for the lateral error. Also, the MPC objective function penalizes ω_s whereas $T_{\rm comp}$ tries to reduce the lateral offset from the center line, which leads to larger values of ω_s. It looks like there are specific, optimal

values for t_s and t_h to achieve good performance. For our case, these are $t_s = 0.5$ sec, and $t_h = 2.0$ sec, which correspond very well to normal human driver response and prediction times.

Another way to interpret the results of Fig. 8 is to observe that if the optimization frequency is high, T_{ant} can prevent ω_s from decreasing. If the optimization frequency is low, there is enough time for T_{comp} to reduce ω_s. However, if the optimization frequency is too low the driver cannot cope with the changes of the environment well. This corresponds to the result of the model with $t_s = 2$ sec in Fig. 8a. Also, the reason why longer t_h does not necessarily result in better performance is that the model tries to satisfy the boundary condition (7) just at t_h, but the ω_s term in the objective function (9) reduces the changing rate of the vehicle heading angle. Thus, the greater t_h, the longer time the controller takes to achieve the boundary condition. This leads to a driver model that may stay away from the center line if the compensatory part is not very effective.

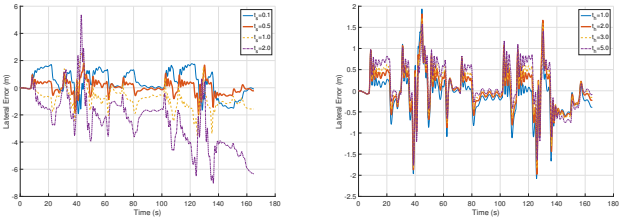

(a) (b)

Fig. 8: The history of lateral error with different settings of t_s with fixed $t_h = 2.0$ sec (left) and with different settings of t_h with fixed $t_s = 0.5$ sec (right).

V. Conclusion

This paper proposes a new driver model with the aim of improving current transfer function-based driver models. The new model is based on the sensorimotor two-point visual driver model, and incorporates MPC in its anticipatory control channel. The resulting system is a hybrid of a discrete-time controller and a continuous-time controller.

We designed this model to overcome difficulties of previous models, namely, explicitly representing the human's anticipating behavior in previous driver models. In order to evaluate the performance of this new model, we conducted several numerical simulations. The proposed model succeeded in a) reproducing the tendency human drivers have, and b) showing equivalent performance to a fully MPC-based model with much less optimization frequency. Parametric studies were conducted to investigate the effect of the sampling period and the prediction horizon to the performance of the overall system. In the future, we plan to investigate the behavior of this model for other driving tasks, such as lane-changing maneuvers.

ACKNOWLEDGMENT

This work was supported by the National Science Foundation awards CMMI-1234286 and CPS-1544814. K. Okamoto was also supported by Funai Foundation for Information Technology.

References

[1] J. J. Gibson and L. E. Crooks, "A theoretical field-analysis of automobile-driving," *The American Journal of Psychology*, pp. 453–471, 1938.

[2] P. Cacciabue, *Modeling Drier Behavior in Automotive Environments*. Springer London, 2007.

[3] D. D. Salvucci and R. Gray, "A two-point visual control model of steering," *Perception*, vol. 33, no. 10, pp. 1233–1248, 2004.

[4] C. Sentouh, P. Chevrel, F. Mars, and F. Claveau, "A sensorimotor driver model for steering control," in *Proceedings of IEEE International Conference on Systems, Man, and Cybernetics*, San Antonio, TX, October 11–14 2009, pp. 2462–2467.

[5] S. Zafeiropoulos and P. Tsiotras, "Design and evaluation of a lane-tracking driver steering assist system with a two-point visual driver model," in *Proceedings of the American Control Conference*, Portland, OR, June 4–6 2014, pp. 3911–3917.

[6] L. Saleh, P. Chevrel, F. Claveau, J.-F. Lafay, and F. Mars, "Shared steering control between a driver and an automation: stability in the presence of driver behaviour uncertainty," *IEEE Transactions on Intelligent Transportation Systems*, vol. 14, no. 2, pp. 974–983, 2013.

[7] D. M. Wolpert, R. C. Miall, and M. Kawato, "Internal models in the cerebellum," *Trends in Cognitive Sciences*, vol. 2, no. 9, pp. 338–347, 1998.

[8] T. Kumagai, Y. Sakaguchi, M. Okuwa, and M. Akamatsu, "Prediction of driving behavior through probabilistic inference," in *Proceedings of the 8th International Conference on Engineering Applications of Neural Networks*, Malaga, Spain, September 8–10 2003, pp. 117–123.

[9] N. Oliver and A. P. Pentland, "Driver behavior recognition and prediction in a smartcar," in *Proceedings of the SPIE 4023, Enhanced and Synthetic Vision 2000*, May 12 2000, pp. 280–290.

[10] A. Pentland and A. Liu, "Modeling and prediction of human behavior," *Neural Computation*, vol. 11, no. 1, pp. 229–242, 1999.

[11] J. Lu, D. Filev, K. Prakah-Asante, F. Tseng, and I. V. Kolmanovsky, "From vehicle stability control to intelligent personal minder: Real-time vehicle handling limit warning and driver style characterization," in *IEEE Workshop on Computational Intelligence in Vehicles and Vehicular Systems*, Nashville, TN, March 30 – April 2 2009, pp. 43–50.

[12] M. Kuderer, S. Gulati, and W. Burgard, "Learning driving styles for autonomous vehicles from demonstration," in *Proceedings of the IEEE International Conference on Robotics and Automation*, Seattle, WA, May 26–30 2015, pp. 2641–2646.

[13] S. D. Keen and D. J. Cole, "Steering control using model predictive control and multiple internal models," in *Proceedings of the 8th International Symposium on Advanced Automotive Control*, Taipei, Taiwan, August 20–24 2006, pp. 783–788.

[14] G. Prokop, "Modeling human vehicle driving by model predictive online optimization," *Vehicle System Dynamics*, vol. 35, no. 1, pp. 19–53, 2001.

[15] H. Wei, W. Ross, S. Varisco, P. Krief, and S. Ferrari, "Modeling of human driver behavior via receding horizon and artificial neural network controllers," in *52nd IEEE Conference on Decision and Control*, Florence, Italy, December 10–13 2013, pp. 6778–6785.

[16] R. Goebel, R. G. Sanfelice, and A. R. Teel, *Hybrid Dynamical Systems: Modeling, Stability, and Robustness*. Princeton University Press, 2012.

[17] M. F. Land and D. N. Lee, "Where do we look when we steer." *Nature*, vol. 369, no. 6483, pp. 742–744, 1994.

[18] A. Bemporad, "Hybrid Toolbox - User's Guide," 2004, http://cse.lab.imtlucca.it/~bemporad/hybrid/toolbox.

[19] Mechanical Simulation Inc., "Carsim," 2009. [Online]. Available: www.carsim.com

[20] E. C. Hildreth, J. M. Beusmans, E. R. Boer, and C. S. Royden, "From vision to action: experiments and models of steering control during driving." *Journal of Experimental Psychology: Human Perception and Performance*, vol. 26, no. 3, pp. 1106–1132, 2000.